Development of a highly sensitive, quantitative, and rapid detection system for Plasmodium falciparum-infected red blood cells using a fluorescent blue-ray optical system

Development of a highly sensitive, quantitative, and rapid detection system for *Plasmodium falciparum*-infected red blood cells using fluorescent blue-ray optical system

Takeki Yamamoto[a, c], Shouki Yatsushiro[b], Muneaki Hashimoto[b], Kazuaki Kajimoto[b], Yusuke Ido[b], Kaori Abe[b], Yasuyuki Sofue[c], Takahiro Nogami[c], Takuya Hayashi[c], Kenji Nagatomi[c], Noboru Minakawa[d], Hiroaki Oka[c], Toshihiro Mita[a, *], and Masatoshi Kataoka[b, *]

[a]Department of Tropical Medicine and Parasitology, Juntendo University School of Medicine, 2-1-1 Hongo, Bunkyo-ku, Tokyo 113-8421, Japan
[b]Health Research Institute, National Institute of Advanced Industrial Science and Technology (AIST), Hayashi-cho 2217-14, Takamatsu 761-0395, Japan
[c]Automotive & Industrial Systems Company, Panasonic Co., 1006 Ooaza-Kadoma, Kadoma, Osaka 571-8506, Japan
[d]Institute of Tropical Medicine, Nagasaki University, 1-12-4 Sakamoto, Nagasaki 852-8523, Japan

Running head: Blue-ray optical system for malaria diagnosis

*Corresponding authors: Masatoshi Kataoka, Biomarker Analysis Group, Health Research Institute, National Institute of Advanced Industrial Science and Technology (AIST),2217-14 Hayashi-cho, Takamatsu 761-0395, Kagawa, Japan
Tel: +81-87-869-3576, Fax: +81-87-869-3553, E-mail: m-kataoka@aist.go.jp and Toshihiro Mita, Department of Molecular and Cellular Parasitology, Juntendo University School of Medicine, 2-1-1 Hongo, Bunkyo-ku, Tokyo 113-8421, Japan
Tel: +81-3-5802-1042, Fax: +81-3-5800-0476, E-mail: tmita@juntendo.ac.jp

Abstract

A highly sensitive diagnostic system for determining low-density infections that are missed by the conventional methods is necessary to detect the carriers of *Plasmodium falciparum*. A fluorescence blue-ray optical system with a scan disc was developed to detect *P. falciparum*-infected red blood cells (*Pf*-iRBCs). The disc was composed of polycarbonate and could analyze nine samples simultaneously. Cultured *P. falciparum* strain 3D7 was used to examine the potential of the system for diagnosing malaria. After an RBC suspension had been applied to the disc, the cells were dispersed on the disc by slight rotation. During the 10 min standing period to allow the RBCs to settle on the disc surface, the cells were simultaneously stained with nuclear fluorescence staining dye Hoechst 34580, which was previously adsorbed on the disc surface. Then, RBCs were arranged on the disc surface as a monolayer by removing excess cells through momentary rotation. Over 1.1 million RBCs remained on the disc for fluorescence analysis. A portable, battery-driven fluorescence image reader was employed to detect fluorescence-positive RBCs for approximately 40 min. A good correlation between examination by conventional light microscopy examination of Giemsa stained RBCs and the developed system was demonstrated over the parasite concentration range of 0.0001%–1.0% by linear regression analysis (R2=0.99993).

The limit of detection was evaluated at 0.00020%. Our results demonstrate the potential of the fluorescence blue-ray optical system for the detection of sub-microscopic low-density *Pf*-iRBCs and accurate quantitative evaluation with extremely easy operation.

Key words: malaria diagnosis, compact disc, highly sensitive detection, *Plasmodium falciparum*

1. Introduction

Malaria, a mosquito-borne infectious disease, is one of the major human infectious diseases, with an estimated 216 million clinical cases and 445,000 deaths in 2016 (World Health Organization, 2017). Light microscopic examination of red blood cells (RBCs) stained with Giemsa stain is recognized as the gold standard for malaria diagnosis, and it remains widespread as a point-of-care diagnostic procedure in clinical and epidemiological settings (Wu et al., 2015). The procedure for light microscopic examination consists of several steps: collection of finger-prick blood, preparation of thin and thick blood smears, staining with Giemsa stain, and quantitative detection of malaria parasites in the RBCs by microscopic examination. However, this microscopic examination is time consuming, and its accuracy depends on the operator's skill. According to the results of British laboratories submitted to the Malaria Reference Laboratory, most routine diagnostic laboratories generally achieved a low detection sensitivity [average, 0.01% parasite concentration (parasitemia)] (Milne et al., 1994). Even under optimal conditions for the detection of malaria parasites with excellent blood preparation and skilled technicians, the detection sensitivity is reported to be low (0.001% parasitemia, corresponding to 50 parasites per microliter), and approximately 1

h is required for the examination (Moody, 2002; Warhurst and Williams, 1996). Antibody-based rapid diagnosis tests (RDT) are often used for malaria diagnosis (Ragavan et al., 2018). Although RDTs have been developed for malaria diagnosis with ease of operation and rapid diagnosis time, the possibility of false-positive and/or false-negative results is a well-known disadvantages of RDTs. The detection sensitivity is similar to that obtained by microscopic examination (McMorrow et al., 2011). Furthermore, several studies revealed that the sensitivity of HRP2-based RDTs could be compromised due to genetic polymorphism of *P. falciparum* HRP2 (Atroosh et al., 2015; Deme et al., 2014; Pava et al., 2010). The sensitivities of light microscopic examination and/or RDT are insufficient for the detection of asymptomatic carriers of *P. falciparum* (Cook et al., 2015; Tiono et al., 2014). Sub-microscopic, low-density malaria infections are considered potential contributors as carriers for ongoing transmission (WHO, 2014, Wu et al., 2015).

High sensitivity of several orders of magnitude for detection of malaria parasites than that of microscopy and RDTs can be achieved by nucleic acid amplification (NAA) techniques such as nested PCR (WHO 2014). However, the disadvantages of NAA tests are that they require multi-step analysis, time-consuming, not quantitative, require costly equipment for analysis and skilled personnel for operation, and lack of onsite

applicability. Microfabrication techniques are expected to be applied in the field of biomedical analysis (Conde et al., 2016). Peng et al. (2014) reported the use of micromagnetic resonance relaxometry for rapid and label-free detection of malaria parasites. Recently, a label-free microfluidic cell deformability sensor for quantitative and high-throughput measurement of malaria parasites has been developed (Yang et al., 2017). However, these devices have not been put into practical use in the field.

In previous studies, we developed a highly sensitive, accurate and quantitative malaria parasite detection system using a cell microarray chip made of polystyrene with 20,944 individually addressable microchambers (Yatsushiro et al., 2010; Yatsushiro et al., 2016). This cell microarray chip was developed to allow the regular dispersion of RBC suspension with a nucleus-staining fluorescence dye in the microchambers with the formation of a monolayer. The potential of this cell microarray chip system for malaria diagnosis was demonstrated by means of monolayer formation of RBCs stained with fluorescence nuclear staining dye and a fluorescence detector equipped with a CCD camera for the detection of fluorescence-positive *Plasmodium falciparum*-infected RBCs (*Pf*-iRBCs). Although it only required less than 30 min for analysis per one sample, several steps for handling of this system and power supply for CCD camera are necessary for malaria diagnosis. For use in a remote area, a diagnostic system with

ease of operation and independent power supply is necessary. Therefore, in the present study, we developed a system with exceptionally higher sensitivity than that of light microscopic examination; the current battery-driven, fluorescence blue-ray optical system with a scan disc was compact and easy to operate (Fig. 1). After sample application on the scan disc, monolayer formation of RBCs and fluorescent nuclear staining of *Pf*-iRBCs could be performed automatically. Then, *Pf*-iRBCs could be quantitatively detected using an image reader in a short time.

2. Materials and Methods

2.1 Construction of the scan disc

The scan disc (EZBNPC01AT, Panasonic Corp. Osaka, Japan; Fig. 2) was constructed from two components, viz., a flow-path disc (Fig. 2A) and an optical disc (Fig. 2B), and each component was made of polycarbonate by general injection molding. Nine compartmentalized portions were formed by bonding the former with the latter by UV curable adhesion patterned by screen printing method (Lee et al., 2009), thereby allowing nine samples to be analyzed simultaneously on the scan disc. For staining

malaria parasites on the scan disc, 180 μl of 0.396 μM Hoechst 34580 (Molecular Probes Inc., Eugene, OR, USA), which is a nuclear-specific fluorescence dye (excitation, 392 nm; emission, 440 nm), was injected into each compartmentalized portion of the scan disc and was allowed to be adsorbed at the detection area through lyophilization for storing at room temperature (Fig. 2D).

The fluorescent material G3300 (Central Techno Corporation, Osaka, Japan) which emits fluorescence at the excitation light of 400 nm, was mixed in the polycarbonate of the flow path disc. When the scan disc was irradiated with light at 400 nm, which yields strong adsorption peak of hemoglobin (Li et al., 2014), RBCs absorbed excitation light, but other part than RBCs adhesion on the scan disc emitted fluorescence. The presence of G3300 in the flow path disc makes it possible to visualize unstained RBCs on the scan disc. This enabled us to distinguish between the fluorescence spots due to nuclear staining dye in the RBCs as *Pf*-iRBCs and the fluorescence spots out of RBCs as detection noises, contributing to an improvement in detection accuracy.

2.2 Construction of the fluorescent image reader

The fluorescence image reader (EZBLMOH01T, Panasonic Corp.) was composed

of a tablet personal computer (PC) and the main body (Fig. 3A, B). The main body included an optical disc drive and field-programmable gate array (FPGA) circuit board. Motions control software (EZBLMO01T-M, Panasonic Corp.) operated the movement of the optical drive and optical pick-up (OPU) via FPGA board (Fig. 3B.1, 2). After OPU moved from the standby position to the measuring position, the scan disc set on the image reader was centrifuged by the motor in the disc drive for scanning. The laser in OPU focused on the surface of the disc and irradiated excitation light. The laser in OPU emitted light at 405 nm, which is similar to the blue-ray system, as excitation light, and the light was focused on the optical disc through an objective lens, the spot diameter of which was 0.5 μm at focal point (Fig. 3C). The optical disc has a pitch of the groove and groove to groove of 0.5 μm, and the optical focal point is positioned along the groove by conventional focal position adjustment method on the optical disc by the servo method (Bouwhuis et al., 1985). The excitation light scanned the whole detection area to acquire image data at intervals of 0.5 μm from each other. Each image dataset was acquired during each scan of the scan disc. With these specifications, a resolution of 0.5 μm was achieved. Fluorescent signals from the disc and/or fluorescent-stained *Pf*-iRBCs were received by an avalanche photodiode (APD), a light receiving element mounted in the OPU. All acquired image datasets were

precisely aligned and signal two-dimensional image of whole detection area was constructed by connecting each image dataset (Fig. 3D, E). Alignment of image data was performed on a PC (Fig. 3B.4) via FPGA circuit board (Fig. 3B.3). With these techniques, it was possible to acquire a high-definition fluorescence image of the whole detection area in a short time as compared with a general fluorescence microscope. The number of RBCs and malaria parasites present in RBCs on the created image were calculated using EZBLMOS01T-A image processing software (Panasonic, Corp.) (Fig. 3B.5).

2.3 Malaria culture

P. falciparum 3D7 cells were cultured in RPMI 1640 medium (Nacalai Tesque, Inc., Tokyo, Japan) supplemented with 50 μg/ml gentamycin (SIGMA-Aldrich Co., St. Louis, MO, USA) and 10% O^+ human serum at a hematocrit of 3%, according to an established method (Trager and Jensen, 1976). Human RBCs (blood group O^+) were obtained from the Japanese Red Cross Society. Parasitemia was calculated by determining the number of *Pf*-iRBCs in 3,000 RBCs and expressed as the ratio to the number of total RBCs. RBCs exhibiting 0.1% parasitemia were added to each plate in 10 ml of culture medium to obtain a final hematocrit of 3%. The plates were then

incubated at 37 °C under 5% CO_2, and 90% N_2 gas.

For light microscopic examination of *Pf*-iRBCs, 2 μl of malaria culture was smeared to make a thin film on each slide, which was then stained with 5% Giemsa (Merck Co. Ltd., Germany) stain in phosphate-buffered saline (pH 7.2). Thereafter, the slide was examined under a light microscope (Olympus, Co., Ltd., Tokyo, Japan), at a magnification of 1,000× to determine the presence or absence of malaria parasites per 3,000 RBCs (Payne, 1988).

2.4 Detection of *Pf*-iRBCs on the scan disc

For analyzing cultured *Pf*-iRBCs on the scan disc, an appropriate volume of purified *Pf*-iRBCs suspension was added to PBS to obtain 0.1% and 1.0% parasitemia at a hematocrit of 0.25%. Parasitemia was examined by thin-smear microscopy with Giemsa staining as described previously (Payne, 1988). To obtain 0.0001%–0.01% parasitemia samples, serial 10-fold dilution of 0.1% parasitemia samples with PBS at a hematocrit of 0.25% was performed. For analysis on the scan disc, 180 μl of the prepared cultured *Pf*-iRBCs was applied to each sample reservoir (Fig. 1A, B). Then, the scan disc was placed against the fluorescence image reader (Fig. 1C). After the "analyze" button was pushed, the following steps were performed automatically:

momentary rotation of the scan disc at 1,000 rpm for 30 s to introduce *Pf*-iRBC suspension from the sample reservoir into the detection area; 10-min standing to allow the RBCs to settle onto the disc surface, during which time the RBCs were simultaneously stained with Hoechst 34580 that had been previously adsorbed on the surface of the detection area; removal of excess RBCs by rotation of the disc at 2,000 rpm for 1 min to form a monolayer of RBCs over the entire surface of the detection area; and finally, fluorescence detection of *Pf*-iRBCs at the detection area (Fig. 1D-F). Nine samples on a scan disc could be analyzed simultaneously in approximately 40 min. *Pf*-iRBCs were distinguished from uninfected RBCs by the fluorescence intensity and size of the fluorescent spot. These fluorescence parameters of individual RBCs were analyzed with the included image processing software. RBCs that exhibited fluorescence intensities that were 1.4–2.4 -times higher than those of uninfected RBCs and having a fluorescent spot size from 1.0 μm^2 to 10 μm^2 were considered to be *Pf*-iRBCs. When the aspect ratio of the fluorescent spot was above 2.4 or its area was below 1.0 μm^2 or above 10 μm^2, this case was noted to be detection noise. Therefore, the numbers of RBCs and *Pf*-iRBCs were calculated automatically by using the software to determine parasitemia. The percentage of parasitemia in each sample was determined as follows: number of *Pf*-iRBCs/total number of RBCs x 100. For the

discrimination of *Pf*-iRBCs from leukocytes on the scan disc, we employed whole blood from a healthy volunteer to examine the fluorescence intensities and sizes of leukocytes for the analysis.

3. Results and Discussion

3.1 Dispersion and monolayer formation of RBCs on the scan disc

The RBC suspension in the sample reservoir of the scan disc was introduced into the detection area through momentary rotation of the disc (Fig. 3A), and the RBCs then settled under gravitational force and adhered on the disc surface as multilayers during 10 min of standing. After rotating the scan disc at 2000 rpm for 1 min, a relatively sparsely formed monolayer of RBCs was observed at the detection area (Figs. 4A- C). The number of dispersed RBCs in the detection area was determined to be 1169623.7 ± 98909 (mean ± standard deviation; n = 67, Fig. 4D). Thus, over 1.1 million RBCs per analysis could be examined for the presence of malaria parasites.

3.2 Detection of *Pf*-iRBCs on the scan disc

To identify *Pf*-iRBCs, differential interference-contrast microscopic examination as described previously was employed (Gruring et al., 2011). Differential interference-contrast microscopic images of *Pf*-iRBCs (Fig. 5A), leukocytes (Fig. 5B), and non-infected RBCs (Fig. 5C) corresponding to conventional fluorescent microscopic images are shown in Figs. 5 D-F. Fluorescence-positive *Pf*-iRBC stained with Hoechst 34580 on the scan disc are shown in Figs. 5G and J, and their fluorescence intensity was evidently lower than that of the leukocyte (Figs. 5H, J). Non-infected RBCs exhibited very weak fluorescent intensities (Figs. 5I, L). Analysis using an image reader allowed examination of fluorescent intensity and fluorescent spot size. Fluorescence- positive *Pf*-iRBC (Fig. 5G) was easily distinguished from leukocyte (Fig. 5H). Then, quantitative analysis of *Pf*-iRBCs and RBCs was performed using an image processing process. The differences in fluorescence intensities must be due to the AT contents in each cell. For the detection of *Pf*-iRBCs on the scan disc, we employed Hoechst 34580, a nuclear-specific fluorescence dye that binds to the minor grove of the AT sequence of DNA. The AT content in the leukocytes was estimated to be approximately 200-times higher than that of *P. falciparum* (Dolezel and Greihuber, 2010; Gardner et al., 2002). Non-infected RBCs do not have a nucleus and, hence, were not stained.

3.3 Quantification of parasitemia

As shown in Fig. 6, linear regression analysis of estimated parasitemia obtained by the fluorescent blue-ray optical system and Giemsa microscopy (1.0, 0.1, 0.01, 0.001, and 0.0001%) revealed a significant relationship (R2=0.99993). Data were expressed as the mean ± standard deviation for seven different experiments. An estimate of the parasitemia is of immediate value to the clinician for the determination of treatment policy and/or prognostication, particularly in the case of *P. falciparum* infection. The limit of detection (LOD) for parasitemia, which yields a signal at $3\sigma/S$ [where σ is the standard deviation of blank solutions (n=32) and S is the slope of calibration curve (Marella et al., 2018)] was 0.00020% (10 parasites/μl), which was an exceptionally highly sensitive than that obtained by microscopic examination of blood smears with Giemsa staining. Nested-PCR is often used for the detection of sub-microscopic, low-density malaria infections. LOD of the developed system was almost compatible with that of nested-PCR (10−50 parasites/μl) (Wang et al., 2014). For malaria elimination, it is necessary to interrupt transmission, which requires identification and treatment of malaria parasite carriers, both symptomatic and asymptomatic (Britton et al., 2016). Although the minimum number of parasites per microliter of whole blood that perpetuates transmission remains uncertain (Britton et al, 2016), sub-microscopic,

low-density malaria infections are considered as potential contributors to ongoing transmission (WHO, 2014, Wu et al., 2015). The current developed fluorescent blue-ray optical system can be employed for the detection of sub-microscopic, low-density infections that are missed by conventional light microscopy and/or RDTs. Furthermore, our developed system is portable, easy to operate, and battery-driven for 6 h. We have shown the potential of the current fluorescent blue-ray optical system for malaria control through quantitative and highly sensitive detection of low-density infections in remote areas.

4. Conclusion

In this study, we developed a potential nuclear fluorescent staining method for exceptionally highly sensitive and quantitative detection of *Pf*-iRBCs in the RBC monolayer formed on the scan disc. Automatic fluorescence analysis can be performed after applying and enclosing the sample on the scan disc to prevent exposure of the blood samples to the end user. This developed system is rather applicable on field. However, the removal of leukocytes from whole blood is necessary prior to application of samples on the scan disc. In a previous study, we developed a push

column with silicon oxide (SiO_2) nano-fibers to separate leukocytes from whole blood (Yatsushiro et al., 2016). We will, thus, employ this push column with SiO_2 nano-fibers in a future prospective experimental study utilizing our current fluorescent blue-ray optical system for malaria diagnosis in the field.

Acknowledgement

This research was supported by AMED under Grant Number JP15km0908001 and by the Global Health Innovative Technology Fund (G2015-210).

Conflict of interest

The authors declare no conflict of interest.

References

Ashley, E.A., Pyae Phyo, A., Woodrow, C.J., 2018. Malaria. Lancet 391, 1608-1621.

Atroosh, W.M., Al-Mekhlafi, H.M., Al-Jasari, A., Sady, H., Al-Delaimy, A.K., Nasr, N.A., Dawaki, S., Abdulsalam, A.M., Ithoi, I., Lau, Y.L., Fong, M.Y., Surin, J., 2015. Genetic variation of pfhrp2 in *Plasmodium falciparum* isolates from Yemen and the performance of HRP2-based malaria rapid diagnostic test. Parasit. Vectors 8, 388.

Bouwhuis, G., Braat, J., Huijser, A., Pasman, J., van Rosmalen, G., Schouhamer I.K., 1985. Principles of optical disc systems. Adam Hilger Ltd, Bristol.

Britton, S., Cheng, Q., McCarthy, J.S., 2016. Novel molecular diagnosis tools for malaria elimination: a review of options from the point of view of high-throughput and applicability in resource limited setting. Malar. J. 15, 88.

Conde, J.P., Madaboosi, N., Soares, R.R., Fernandes, J.T., Novo, P., Moulas, G., Chu, V., 2016. Lab-on-chip systems for integrated bioanalysis. Essays Biochem. 60, 121-131.

Cook, j., Xu, W., Msellem, M., Vonk, M., Bergstrom, B., Gosling, R., Al-Mafazy, A.W., McElroy, P., Molteni, F., Abass, A.K., Garimo, I., Ramsan, M., Ali, A., Martensson, A., Bjorkman, A., 2015. Mass screening and treatment on the basis of results of a *Plasmodium falciparum*-specific rapid diagnosis test did not reduce malaria incidence in Zanzibar. J. Infect. Dis. 211, 1476-1483.

Carlton, J.M., Angiuoli, S.V., Suh, B.B., Kooij, T.W., Pertea, M., Silva, J.C., Ermolaeva, M.D., Allen, JE, Selengut, J.D., Koo, H.L., Peterson, J.D., Pop, M., Kosack, D.S., Shumway, M.F., Bidwell, S.L., Shallom, S.J., van Aken, S.E., Riedmuller, S.B., Feldblyum, T.V., Cho, J.K., Quackenbush, J., Sedegah, M., Shoaibi, A., Cummings, L.M., Florens, L., Yates, J.R., Raine, J.D., Sinden, R.E., Harris, M.A., Cunningham, D.A., Preiser, P.R., Bergman, L.W., Vaidya, A.B., van Lin, L.H., Janse, C.J., Waters, A.P., Smith, H.O., White, O.R., Salzberg, S.L., Venter, J.C., Fraser, C.M., Hoffman, S.L., Gardner, M.J., Carucci, D.J., 2002. Genome sequence of the human malaria parasite *Plasmodium falciparum*. Nature 419, 498-511.

Dolezel, J., Greihuber, J., 2010. Nuclear genome size: are we getting closer? Cytometry A. 77, 635-642.

Deme, A.B., Park, D.J., Bei, A.K., Sarr, O., Badiane, A.S., Gueye, Pel, H., Ahouidi, A., Ndir, O., Mboup, S., Wirth, D.F., Ndiaye, D., Volkman, S.K., 2014. Analysis of pfhrp2 genetic diversity in Senegal and implications for use of rapid diagnosis tests. Malar. J. 13, 34.

Gruring, C., Heiber, A., Kruse, F., Ungefehr, J., Gilberger, T.W., Spiemann, T., 2011. Development and host cell modifications of *Plasmodium falciparum* blood stages in four dimensions. Nat. Commun. 2, 165.

Lee, B.S., Lee, J.N., Park, J.M., Lee, J.G., Kim, S., Cho, Y.K., Ko, C., 2009. A fully automated immunoassay from whole blood on a disc. Lab Chip 9, 1548-1555.

Li, W., Lin, L., Li, G., 2014. Wave selection method based on test analysis of variance: application to oximetry. Anal. Methods 6, 1082-1089.

Marella, V., Lalitha, K., Pravallika, M., Nalluri, B.N., 2018. Novel RP-HPLC Method for the determination of paroxetine in pure form and in tablet formulation. Pharm. Methods 9, 45-48.

McMorrow, M.L., Aidoo, M., Kachur, S.P., 2011. Malaria rapid diagnostic tests in elimination settings--can they find the last parasite? Clin. Microbiol. Infect. 17, 1624-1631.

Milne, L.M., Kyi, M.S., Chiodini, P.L., Warhurst, D.C., 1994. Accuracy of routine laboratory diagnosis of malaria in the United Kingdom. J. Clin. Pathol. 47, 740-742.

Moody, A., 2002. Rapid diagnostic tests for malaria parasites. Clin. Microbiol. Rev. 15, 66-78.

Pava, Z., Echeverry, D.F., Diaz, G., Murillo, C., 2010. Large variation in detection of histidine-rich protein 2 in *Plasmodium falciparum* isolates from Colombia. Am. J. Trop. Med. Hyg. 83, 834-837.

Payne, D., 1988. Use and limitations of light microscopy for diagnosing malaria at the primary health care level. Bull. World Health Organ. 66, 621-626.

Peng, W.K., Kong, T.F., Ng, C.S., Chen, L., Huang, Y., Bhagat, A.A., Nguyen, N.T., Preiser, P.R., Han, J., 2014. Micromagnetic resonance relaxometry for rapid label-free malaria diagnosis. Nat. Med. 20, 1069-1073.

Ragavan, K.V., Kumar, S., Swaraj, S., Neethirajan, S., 2018. Advanced in biosensors and optical assays for diagnosis and detection of malaria. Biosens. Bioelectron. 105, 188-210.

Tiono, A.B., Ouedraogo, A., Diarra, A., Coulibaly, S., Soulama, I., Konate, A.T., Barry, A., Mukhopadhyay, A., Sirima, S.B., Hamed, K., 2014. Lessons learned from the use of HRP-2 based rapid diagnosis test in community-wide screening and treatment of asymptomatic carriers of *Plasmodium falciparum* in Burkina Faso. Malar. J. 13, 30.

Trager, W., Jensen, J.B., 1976. Human malaria parasites in continuous culture. Science 193, 673-675.

Wang, B., Han, S.S., Cho, C., Han, J.H., Cheng, Y., Lee, S.K., Galappaththy, G.N., Thimasarn, K., Soe, M.T., Oo, H.W., Kyaw, M.P., Han, E.T., 2014. Comparison of microscopy, nested-PCR, and real-time-PCR assays using high-throughput screening of

pooled samples for diagnosis of malaria in asymptomatic carriers from areas of endemicity in Myanmar. J. Clin. Microbiol. 52, 1838-1845.

Warhurst, D.C., Williams, J.E., 1996. ACP Broadsheet no 148. July 1996. Laboratory diagnosis of malaria. J. Clin. Pathol. 49, 533-538.

Warhurst, D.C., Williams, J.E., 2004. Laboratory procedures for diagnosis of malaria, in: Abdalla, S.H., Pasvol, G. (Eds.), Malaria. Imperial College Press, pp. 1-27.

WHO, 2014. Global Malaria Program. WHO, Switzerland.

WHO, 2016. World Malaria Report 2017. World Malaria Report. WHO, Switzerland.

Wu, L., van den Hoogen, L.L., Slater, H., Walker, P.G., Ghani, A.C., Drakeley, C.J., Okell, L.C., 2015. Comparison of diagnostics for the detection of asymptomatic *Plasmodium falciparum* infections to inform control and elimination strategies. Nature 528, S86-93.

Yang, X., Chen, Z., Miao, J., Cui, L., Guan, W., 2017. High-throughput and label-free parasitemia quantification and stage differentiation for malaria-infected red blood cells. Biosens. Bioelectron. 98, 408-414.

Yatsushiro, S., Yamamoto, T., Yamamura, S., Abe, K., Obana, E., Nogami, T., Hayashi, T., Sesei, T., Oka, H., Okello-Onen, J., Odongo-Aginya E.I., Alai, M.A., Olia, A., Anywar, D., Sakurai, M., Palacpac, N.M., Mita, T., Horii, T., Baba, Y., Kataoka, M., 2016. Application of a cell microarray chip system for accurate, highly sensitive, and rapid diagnosis for malaria in Uganda. Sci. Rep. 6, 30136.

Yatsushiro, S., Yamamura, S., Yamaguchi, Y., Shinohara, Y., Tamiya, E., Horii, T., Baba, Y., Kataoka, M., 2010. Rapid and highly sensitive detection of malaria-infected erythrocytes using a cell microarray chip. PLoS One 5, e13179.

Figure legends

Figure 1. Schematic depiction of the process for detection of *Pf*-iRBCs using the fluorescent blue-ray optical system. (A) For analysis on the scan disc, 180-μl samples of *Pf*-iRBCs were prepared. (B) *Pf*-iRBCs were applied to each sample reservoir via a pipette. (C) The scan disc was placed against the fluorescence image reader. (D) RBCs were analyzed at the detection area. (E) Monolayer formation of RBCs and nuclear fluorescence staining of *Pf*-iRBCs at the detection area. (F) Fluorescence image of *Pf*-iRBCs on the disc. The target malaria parasites were analyzed quantitatively at the single-cell level (red arrow, malaria parasite).

Figure 2. Construction of the scan disc. The scan disc comprises two components, viz., a flow-path disc (A) and an optical disc (B), each of which is made of polycarbonate. Nine compartmentalized portions are formed by the bonding of the flow-path disc with the optical disc by the UV-curable adhesion method (C). Schematic diagram of a cross section of the scan disc is shown (D).

Figure 3. Construction of the image reader

Overall picture of the image reader is shown (A). Image reader internal components and controller (B). Schematic diagram of the optical system using OPU and acquisition of fluorescence signal from the scan disc (C). Processing of two-dimensional images of the acquired fluorescence data are shown (D). Fluorescence image of *Pf*-iRBC on the scan disc (E).

Figure 4. Monolayer formation of RBCs in the detection area. Monolayer formation of RBCs in the detection area of the scan disc is shown (A). Microscopic images of the detection area are also given (B, C). A sparse monolayer of RBCs at the detection area is evident (C). Histogram plot of the number of dispersed RBCs in the detection area (D).

Figure 5. Discrimination of leukocytes and *Pf*-iRBCs on the fluorescent blue-ray optical system. Differential interference-contrast microscopic images of *Pf*-iRBCs dispersed on the scan disc. *Pf*-iRBC (A), leukocyte (B), and non-infected RBCs (C) are shown. Conventional fluorescence microscopic images of *Pf*-iRBC (D), leukocyte (E), and non-infected RBCs (F) are shown. Fluorescence images of *Pf*-iRBC (G), leukocyte (H), and non-infected RBCs (I) by fluorescence blue-ray image reader. (J-L)

Fluorescence- intensity profile along the yellow-dotted arrow in each image is shown (G-I). Fluorescence image of whole RBCs was darker than that of the disc surface through the mixing of the fluorescence material G3300 in the polycarbonate. Fluorescence intensity of *Pf*-iRBC stained with Hoechst 34580 was apparently higher than that of the disc surface.

Figure 6. Comparative analysis of the estimated parasitemia obtained with the fluorescent blue-ray optical system and conventional Giemsa staining microscopic method. Linear regression analysis was used. The number of fluorescence-positive RBCs was determined for each parasitemia samples. Data were expressed as the mean ± standard deviation for seven different experiments.

Figure 1

Fig. 1

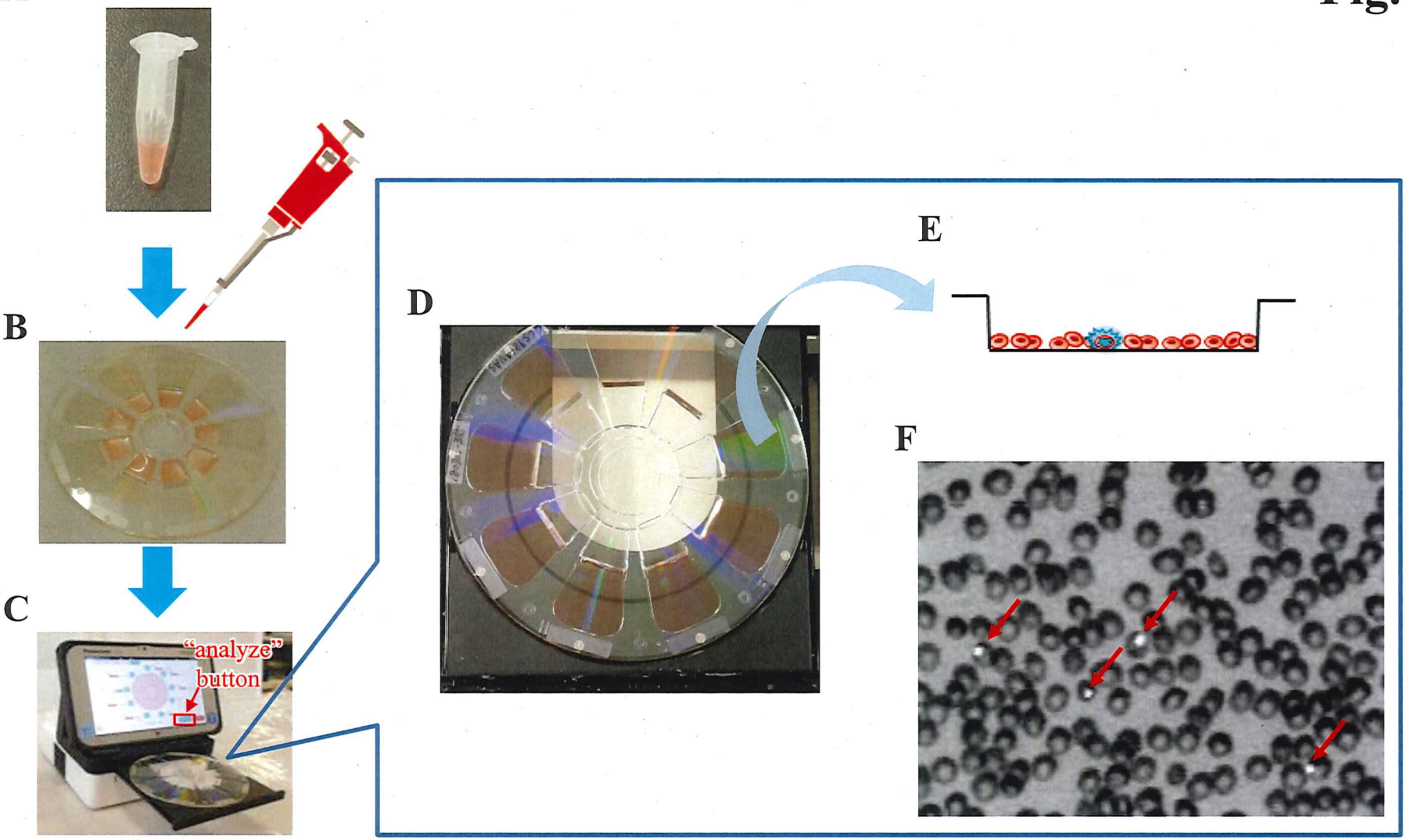

Figure 2

Fig. 2

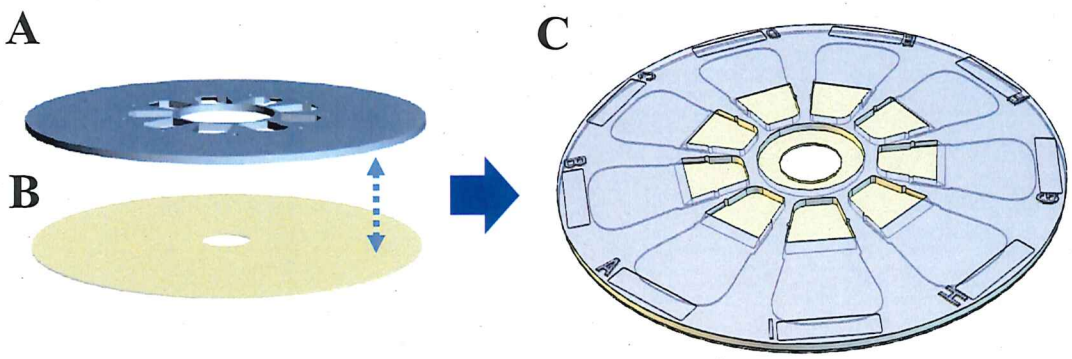

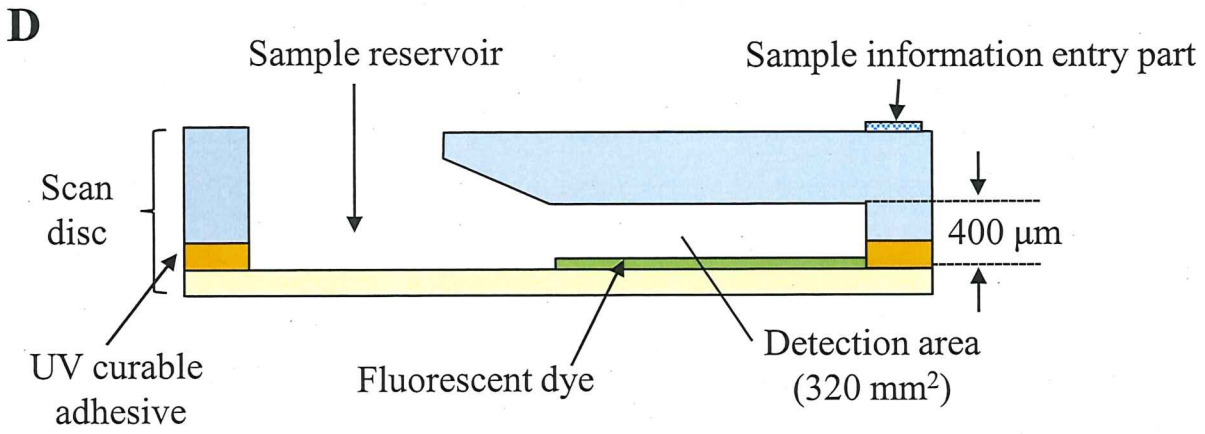

Figure 3

Fig. 3

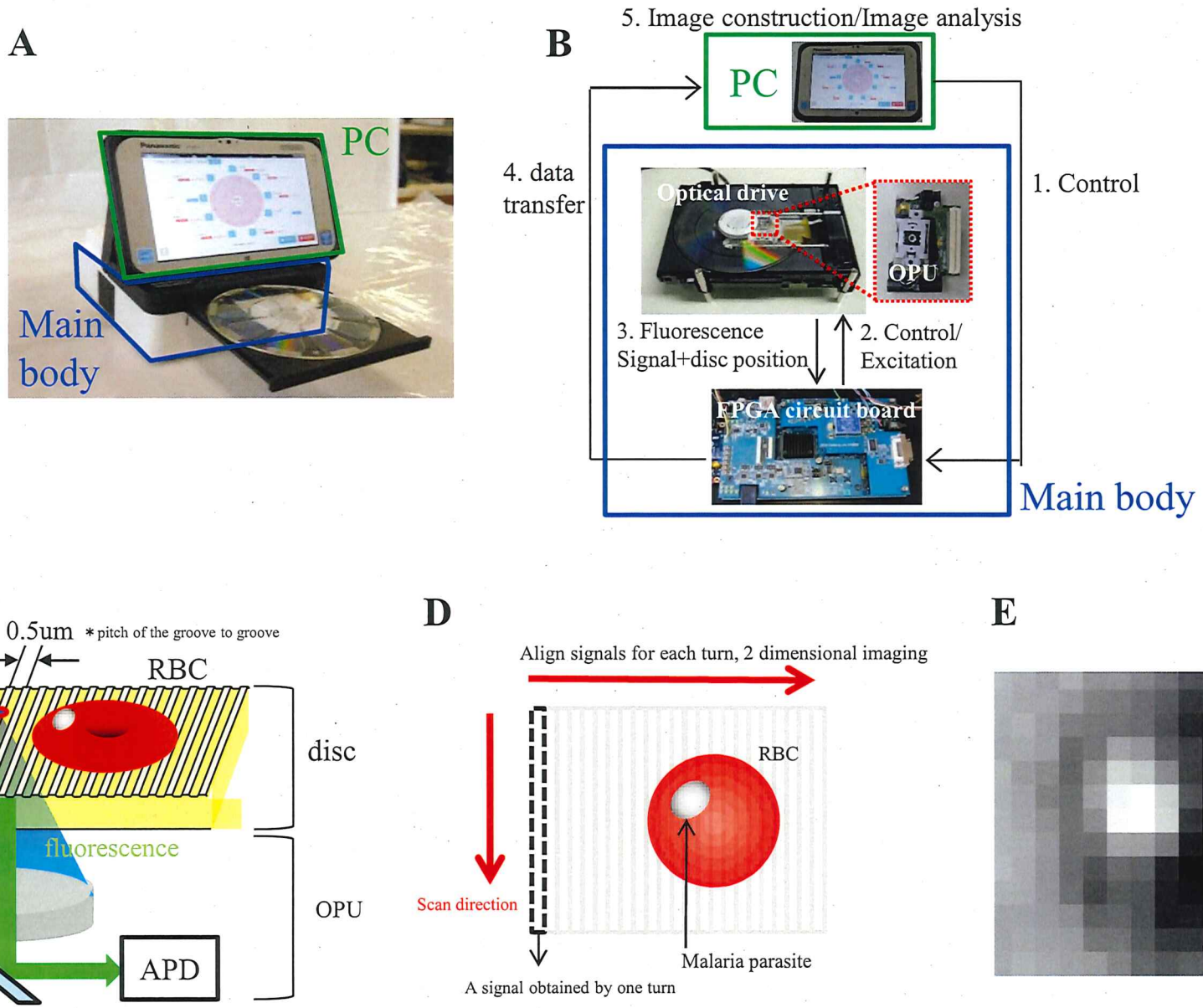

Figure 4

Fig. 4

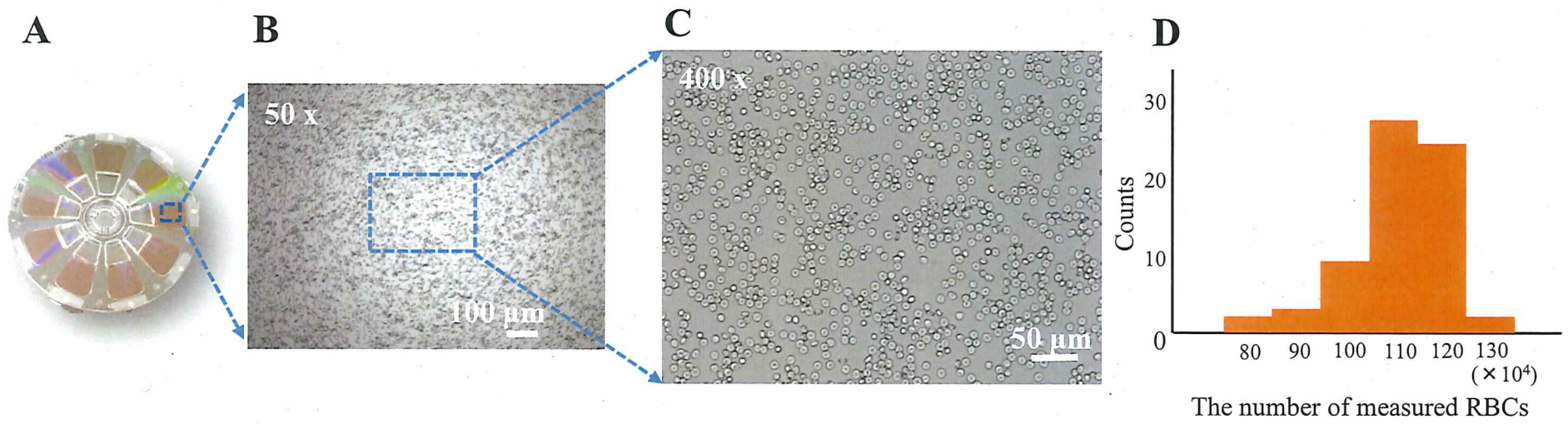

Figure 5

Fig. 5

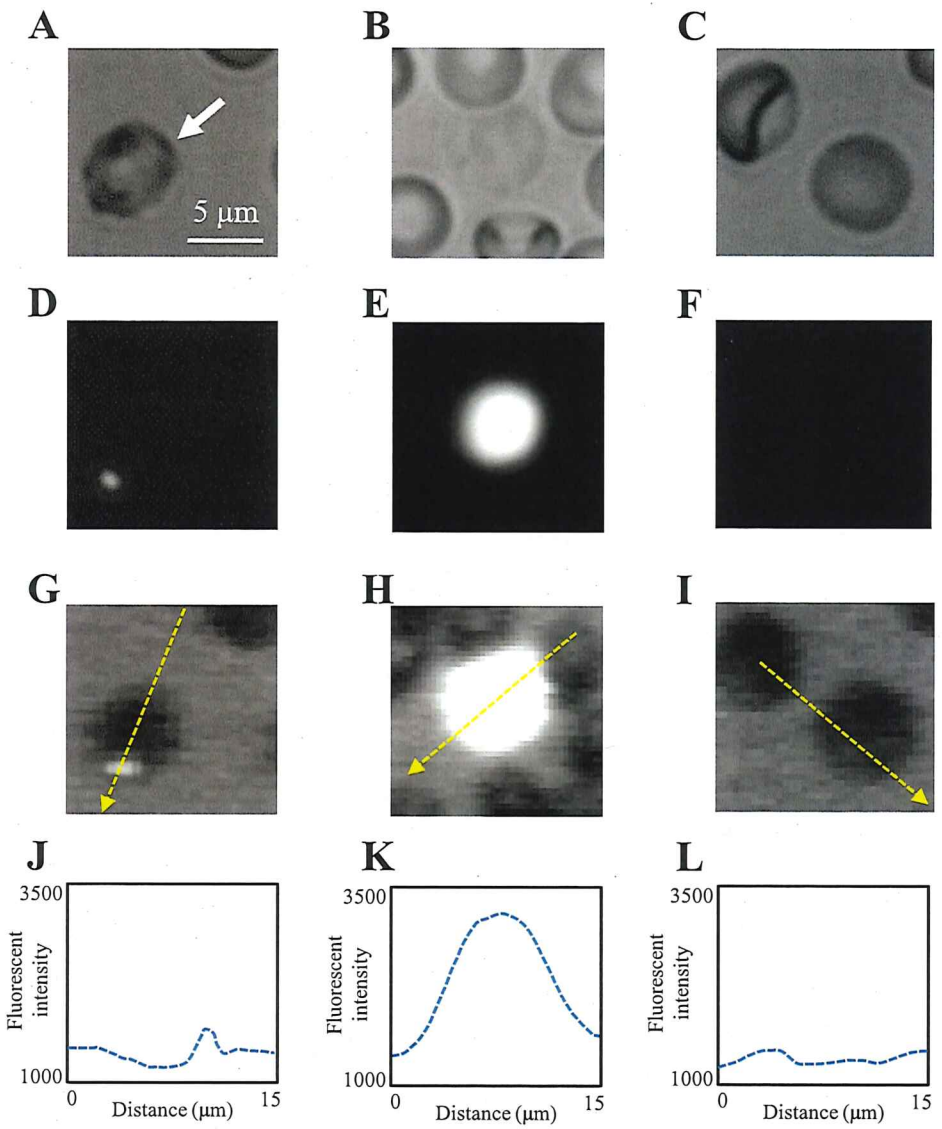

Figure 6

Fig. 6